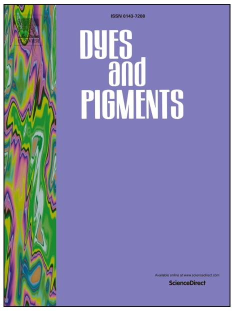

Carbazole-based aggregation-induced emission (AIE)-active gold(I) complex: Persistent room-temperature phosphorescence, reversible mechanochromism and vapochromism characteristics

Zhao Chen, Gang Liu, Shouzhi Pu, Sheng Hua Liu

PII: S0143-7208(17)30175-4

DOI: 10.1016/j.dyepig.2017.05.003

Reference: DYPI 5965

To appear in: *Dyes and Pigments*

Received Date: 26 January 2017

Revised Date: 30 April 2017

Accepted Date: 2 May 2017

Please cite this article as: Chen Z, Liu G, Pu S, Liu SH, Carbazole-based aggregation-induced emission (AIE)-active gold(I) complex: Persistent room-temperature phosphorescence, reversible mechanochromism and vapochromism characteristics, *Dyes and Pigments* (2017), doi: 10.1016/j.dyepig.2017.05.003.

Carbazole-based aggregation-induced emission (AIE)-active gold(I) complex: persistent room-temperature phosphorescence, reversible mechanochromism and vapochromism characteristics

Zhao Chen [a], Gang Liu [a], Shouzhi Pu [a, **], Sheng Hua Liu [b, *]

Synopsis

A carbazole-based gold(I) complex was successfully synthesized. The complex is AIE-active, and it can emit persistent room-temperature phosphorescence. Moreover, the luminogen exhibits reversible mechanochromism and vapochromism characteristics.

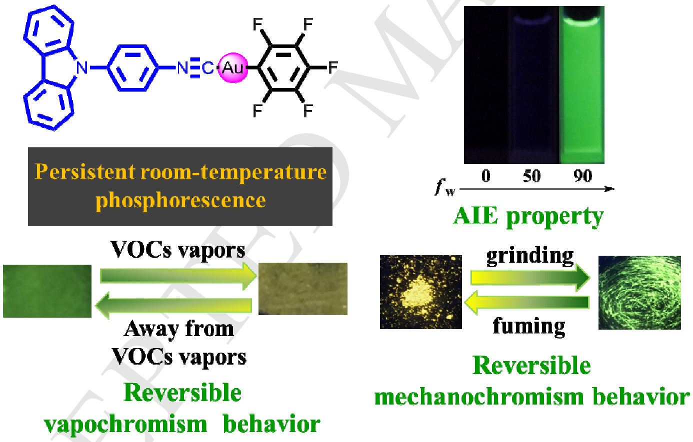

Carbazole-based aggregation-induced emission (AIE)-active gold(I) complex: persistent room-temperature phosphorescence, reversible mechanochromism and vapochromism characteristics

Zhao Chen [a], Gang Liu [a], Shouzhi Pu [a, **], Sheng Hua Liu [b, *]

[a] Jiangxi Key Laboratory of Organic Chemistry, Jiangxi Science and Technology Normal University, Nanchang 330013, PR China.

[b] Key Laboratory of Pesticide and Chemical Biology, Ministry of Education, College of Chemistry, Central China Normal University, Wuhan 430079, PR China.

Tel: +86-791-83831996   Fax: +86-791-83831996

** Corresponding author E-mail: pushouzhi@tsinghua.org.cn

* Corresponding author E-mail: chshliu@mail.ccnu.edu.cn

ABSTRACT

A carbazole-based gold(I) complex **1** has been successfully synthesized. Its structure was characterized by nuclear magnetic resonance spectroscopy, elemental analysis and single crystal X-ray diffractometry. Its aggregation-induced emission behavior was studied by ultraviolet/visible, photoluminescence spectroscopy and scanning electron microscope. Its solid-state mechanochromic and thin-film vapochromic luminescence behaviors were also investigated by photoluminescence spectroscopy. The results demonstrated that luminogen **1** showed obvious aggregation-induced emission property. Furthermore, **1** also exhibited reversible high-contrast mechanochromic and vapochromic luminescence behaviors. More interestingly, **1** can emit persistent room-temperature phosphorescence with a solid-state emission lifetime up to 86.84 ms, which is the highest lifetime value among all the reported gold(I) complexes so far. To the best of our knowledge, the gold(I) complex is the first example of an AIE-active luminogen with persistent room-temperature phosphorescence, reversible mechanochromism and vapochromism characteristics.

Keywords: Gold(I) complex; Carbazole; Aggregation-induced emission; Persistent room-temperature phosphorescence; Mechanochromism; Vapochromism

1. Introduction

The development of efficient luminescent materials has received a great deal of attention both in fundamental science and practical applications [1-3]. Especially, smart luminescent materials responding to external stimuli have attracted increasing interest due to their potential applications in the fields of sensors, security inks and optoelectronic devices [4-8]. Mechanochromic emissive materials, as a class of smart luminescent materials, have aroused widespread concern [9-12]. Vapochromic materials, which involve luminescent changes upon exposure to volatile organic vapors, are also one promising type of smart luminescent materials [13-19]. High aggregative-state emission and obvious color contrast before and after stimulating are two extremely important factors for the highly efficient application of stimuli-responsive smart materials [20]. However, most conventional luminogens commonly show poor aggregate state emission efficiency because of the presence of notorious aggregation caused quenching (ACQ) phenomenon [21], which blocks the effective development of stimuli-responsive materials. Fortunately, a new photophysical process of aggregation-induced emission (AIE) was discovered by Tang *et al.* in 2001 [22]. The luminogens possessing AIE effect can achieve bright luminescence by the aggregate formation. Therefore, it is very significant to synthesize multistimuli-responsive AIE materials with mechanochromism and vapochromism characteristics. Over the past two decades, gold(I) chemistry has aroused the interest of many researchers owing to the occurrence of fascinating aurophilic interactions between gold centers [23-32]. To date, nevertheless, AIE-active gold(I) complexes with mechanochromic and vapochromic behaviors are rather rare [28,30,33-35].

Carbazole-based luminescent materials are valuable candidates in the domain of photoelectronic devices [36-39]. Unfortunately, the ACQ effect hinders the high-efficiency application of these luminescent materials containing carbazole unit. Thus, it is a meaningful research topic to design and synthesize carbazole-based derivatives with AIE property. On the other hand, most phosphorescence-emitting metal complexes with mechanochromism behavior exhibit short phosphorescence lifetimes (< 1 ms) [40-42], and metal complex simultaneously possessing persistent room-temperature phosphorescence and reversible mechanochromism characteristics has yet to be reported, not to mention AIE-active vapochromic gold(I) complex with these intriguing properties. In this work, we described a carbazole-based mononuclear gold(I) complex **1** (Chart 1). AIE, mechanochromism and vapochromism characteristics of the luminogen were systematically investigated. **1** exhibited obvious AIE behavior, Furthermore, **1** also showed reversible high-contrast mechanochromic and vapochromic luminescence. More importantly, **1** can emit persistent solid-state room-temperature phosphorescence with luminescence lifetime up to 86.84 ms.

Insert Chart 1

2. Materials and methods

2.1. Experimental

General: All manipulations were carried out under an argon atmosphere by using standard Schlenk techniques, unless otherwise stated. The starting material carbazole purchased from Alfa Aesar was used as received. CH_2Cl_2 was dried with CaH_2 then distilled. All other starting materials and reagents were obtained as analytical-grade from commercial suppliers and used without further purification. Compound **1-b** [43] and $C_6F_5Au(tht)$ (tht = thiophane) [44] were prepared by procedures described in the corresponding literatures. ^1H NMR (400 MHz) and ^{13}C NMR (100 MHz) spectra were collected on American Varian Mercury Plus 400 spectrometer (400 MHz). ^1H NMR spectra are reported as followed: chemical shift in ppm (δ) relative to the chemical shift of TMS at 0.00 ppm, integration, multiplicities (s = singlet, d = doublet, t = triplet, m = multiplet), and coupling constant (Hz). ^{13}C NMR chemical shifts reported in ppm (δ) relative to the central line of triplet for $CDCl_3$ at 77 ppm. ^{19}F NMR chemical shifts are relative to C_6F_6 (δ = -163.00). EI-MS was obtained using Thermo scientific DSQ II. Elemental analyses (C, H, N) were carried out with a PE CHN 2400 analyzer. Ultraviolet/Visible spectra were obtained on U-3310 UV Spectrophotometer. Fluorescence spectra were recorded on a Hitachi-F-4500 fluorescence spectrophotometer and Fluoromax-P luminescence spectrometer (HORIBA JOBIN YVON INC.). Luminescent decay experiment was measured by Edinburgh FLS980 spectrometer. XRD studies were recorded on a Shimadzu XRD-6000 diffractometer using Ni-filtered and graphite-monochromated Cu Kα radiation (λ = 1.54 Å, 40 kV, 30 mA). The N, N-dimethyl formamide (DMF)/water mixtures with various water fractions were prepared by slowly adding ultra-pure water into the DMF solution of samples. Absolute luminescence quantum yields were measured by HAMAMATSU ABSOLUTE PL QUANTUM YIELD SPECTROMETER C11347. Dynamic light scattering (DLS) measurements were performed on the Zetasizer instrument ZEN3600 (Malvern, UK) with a 173° back scattering angle and He-Ne laser (λ = 633 nm). The X-ray crystal-structure determination of complex **1** was obtained on a Bruker APEX DUO CCD system. The aggregate behavior and the solid-state surface morphology of **1** were investigated by scanning electron microscopy (SEM, Zeiss, Sigma). Column chromatographic separations were carried out on silica gel (200-300 mesh). TLC was performed by using commercially prepared 100-400 mesh silica gel plates (GF254) and visualization was effected at 254 nm.

2.2 Synthesis

*2.2.1 Synthesis of monoisocyano ligand **1-d***

Synthesis of **1-c**: A mixture of compound **1-b** (3.0 g, 11.6 mmol), formic acid (30 ml) were stirred for overnight at 110℃. After completion of present reaction, formic acid was removed from reaction system by distillation, the residual mixture was extracted with dichloromethane (3 × 30 mL), the combined organic layers were washed with brine, dried (Na_2SO_4), and concentrated in vacuo. The residues were purified by column chromatography, affording the expected pale solid product in a yield of 83%. ^{1}H NMR (400 MHz, $CDCl_3$): δ (ppm) = 8.83-8.46 (m, 1H), 8.16-8.13 (m, 2H), 7.77 (d, *J* = 8 Hz, 1H), 7.58-7.52 (m, 2H), 7.44-7.27 (m, 8H). ^{13}C NMR (100 MHz, $CDCl_3$): δ (ppm) = 162.5, 159.1, 140.8, 140.8, 135.9, 135.8, 134.8, 134.0, 128.5, 127.8, 126.0, 126.0, 123.3, 123.3, 121.2, 120.4, 120.3, 120.1, 120.0, 109.6, 109.5. EI-MS: m/z = 286.16[M]$^+$. Anal. Calcd. for $C_{19}H_{14}N_2O$: C, 79.70; H, 4.93; N, 9.78. Found: C, 79.74; H, 4.95; N, 9.75.

Synthesis of **1-d**: A CH_2Cl_2 suspension (15 ml) of **1-c** (1.0 g, 3.5 mmol) and triethylamine (5 ml) was cooled to 0℃. To the mixture was added dropwise a CH_2Cl_2 solution (10 ml) of triphosgene (1.16 g, 3.9 mmol). The mixture was refluxed under an argon atmosphere for 3 h, then 10% aq. Na_2CO_3 (50 ml) was added dropwise at room temperature. the mixture was extracted with dichloromethane (3 × 30 mL). The combined organic layers were washed with brine, dried (Na_2SO_4), and concentrated in vacuo. The residues were purified by column chromatography, affording the expected gray solid product in a yield of 77%. ^{1}H NMR (400 MHz, $CDCl_3$): δ (ppm) = 8.14 (d, *J* = 8 Hz, 2H), 7.63 (s, 4H), 7.45-7.30 (m, 6H). ^{13}C NMR (100 MHz, $CDCl_3$): δ (ppm) = 165.3, 140.2, 138.7, 128.0, 127.7, 126.2, 123.7, 120.6, 120.4, 109.4. EI-MS: m/z = 268.14[M]$^+$. Anal. Calcd. for $C_{19}H_{12}N_2$: C, 85.05; H, 4.51; N, 10.44. Found: C, 85.02; H, 4.55; N, 10.41.

*2.2.2 Synthesis of complex **1** containing mononuclear gold(I) unit*

Synthesis of **1:** A mixture of $C_6F_5Au(tht)$ (0.26 g, 0.57 mmol) and **1-d** (0.15 g, 0.56 mmol) was stirred in CH_2Cl_2 (20 ml) over night under an argon atmosphere at room temperature. After completion of present reaction, the solvent was evaporated. A small amount of CH_2Cl_2 was added, and then a lot of *n*-hexane was added. Collecting the white solid product by suction filtration. Yield = 93%. ^1H NMR (400 MHz, $CDCl_3$): δ (ppm) = 8.15 (d, *J* = 8 Hz, 2H), 7.80 (s, 4H), 7.46-7.34 (m, 6H). ^{19}F NMR ($CDCl_3$): δ (ppm) = -116.60, -157.80, -162.87. Anal. Calcd. for $C_{25}H_{12}AuF_5N_2$: C, 47.49; H, 1.91; N, 4.43. Found: C, 47.56; H, 1.95; N, 4.38.

Insert Scheme 1

3. Results and discussion

3.1. Synthesis

The carbazole-based mononuclear gold(I) complex **1** was prepared according to the corresponding synthetic strategy presented in Scheme 1. The intermediate product **1-d** as starting material reacted with $C_6F_5Au(tht)$ (tht = thiophane) to afford the target gold(I) complex **1** in 93% yield.

3.2. Crystallographic details

Single crystals of complex **1** suitable for X-ray analysis were obtained by slow diffusion of *n*-hexane into its dilute solution of dichloromethane. A crystal of **1** with approximate dimensions of 0.30 × 0.05 × 0.02 mm^3 for **1** was mounted on a glass fiber for diffraction experiment. Intensity data were collected on a Nonius Kappa

CCD diffractometer with Mo Kα radiation (0.71073 Å) at room temperature. The structures were solved by a combination of direct methods (SHELXS-97) [45] and Fourier difference techniques and refined by full-matrix least-squares (SHELXL-97) [46]. All non-H atoms were refined anisotropically. The hydrogen atoms were placed in the ideal positions and refined as riding atoms. Further crystal data are provided in Table S1 (Supporting Information). The selective bond lengths and angles can be found in Table S2 (Supporting Information). Crystallographic data for the structure in this paper have been deposited with the Cambridge Crystallographic Data Centre as supplemental publication CCDC 1516083.

3.3. Aggregation Induced Emission (AIE)

To investigate the aggregation-induced property of luminogen **1**, the ultraviolet (UV)/visible-absorbance spectra of **1** (10 μM) in DMF-H_2O mixtures with different water fractions (f_w) were studied (Supporting Information: Fig. S1). The result demonstrated that the absorption peak of **1** at around 336 nm was red-shifted as the water content was increased. Meanwhile, the absorption spectra exhibited level-off tails in the long-wavelength region as the f_w values were increased. Such spectral tails are caused by the Mie scattering effect, which commonly implies the generation of nanoscopic aggregates [47,48]. As shown in Fig. 1, one emission band with a maximum (λ_{max}) at 395 nm was observed when a dilute DMF solution of **1** was excited at 330 nm, and almost no luminescence was noticed under 365 nm UV light. However, when the water volume fraction in the DMF solution was increased to 50%, **1** showed faint blue luminescence, likely due to the restricted intramolecular rotation of carbazole unit [49]. When the f_w value was 60%, two new emission bands were observed with λ_{max} at 425 nm and 530 nm, and **1** displayed faint yellow-green light emission under 365 nm UV light. At f_w = 90%, the mixture exhibited a strong yellow-green emission. This is because water is a nonsolvent of luminogen **1** and thus aggregation will happen as the increase of the f_w value. Clearly, the bright yellow-green luminescence of **1** can be attributed to the aggregate formation. Indeed, the nano-aggregates obtained were confirmed using dynamic light scattering (DLS). The DLS experimental results indicated the real existence of nano-aggregates. Meanwhile, the size of nano-aggregates became smaller with the f_w increased (Supporting Information: Fig. S2). Furthermore, the aggregate behavior of **1** was also explored via scanning electron microscope (SEM). The SEM image indicated that **1** molecules tended to aggregate in the DMF/H_2O mixture with f_w = 90% (Supporting Information: Fig. S3). Obviously, complex **1** is AIE-active, and its AIE behavior is possibly triggered by the synergistic effects of the restricted intramolecular rotation and the formation of intermolecular gold-gold interactions [50].

Insert Figure 1

*3.4. Reversible Mechanochromism and persistent room-temperature phosphorescence characteristics of complex **1***

The reversible mechanochromic effect of complex **1** was surveyed by solid-state photoluminescence (PL) spectroscopy. As presented in Fig. 2, the as-synthesized solid sample of **1** exhibited strong yellow emission with an absolute luminescence quantum yield up to 22.5% at 462 nm, 550 nm and 598 nm. Intriguingly, a persistent yellow room-temperature phosphorescence could be observed when the 365 nm UV light was turned off (see Movie S1). As evident from Fig. 3, the emission lifetime of **1** was as high as 86.84 ms, which is the highest lifetime value among all the reported gold(I) complexes. In addition, upon gentle grinding of solid sample **1** using a pestle or a spatula, a new emission band with the λ_{max} at 538 nm was visible, and the yellow-green light-emitting powder was formed. Its absolute luminescence quantum yield was 19.8%, and its emission lifetime was 1.44 μs (Supporting Information: Fig. S4). The emission peak at 538 nm is correspond to those observed in DMF/water mixtures with high f_w values. After fuming with dichloromethane solvent vapor for 30 s, the original yellow emitting condition was completely restored. Furthermore, the reversible mechanochromic conversion between yellow and yellow-green emission colors could be repeated many times without fatigue (Fig. 4). The experimental results of SEM showed that the crystal packing of solid sample **1** may readily collapse upon gentle grinding. (Supporting Information: Fig. S5). To gain insight into the mechanochromic mechanism of complex **1**, X-ray diffraction (XRD) measurements of various solid states of **1** were performed. As can be seen in Fig. 5, the as-prepared solid sample showed a lot of sharp and intense diffraction peaks, which indicated its crystalline nature. In contrast, the XRD diffractogram of the ground sample did not exhibit any noticeable reflection peaks, indicative of its amorphous nature. When the yellow-green light-emitting sample was fumigated with dichloromethane solvent vapor, the sharp and intense diffraction peaks coinciding with those in the untreated sample was attained again, suggesting the recovery of the ordered crystalline state. Therefore, the mechanochromic phenomenon observed in coordination compound **1** is associated with the morphological transition between the ordered crystalline phase and the disordered amorphous phase. As shown in Fig. 6, the shortest intermolecular Au···Au distances are 4.699 Å, indicating lack of strong intermolecular aurophilic interactions [51]. In addition, the distances between Au-π are 2.056 Å and 2.049 Å, and the distances between Au-CN are 1.931 Å and 1.982 Å. Furthermore, multiple weak intermolecular C-H··π interactions (*d* = 2.566 Å) as well as C-H···F interactions ($d_{H\cdots F}$= 2.514 Å, 2.586 Å, 2.617 Å) exist in the crystals, which facilitate the molecular packing, suppress free rotation of molecular structure and then promote the formation of long lifetime phosphorescence [52-55]. The emission color of the single crystal is bright yellow, and its emission spectrum is shown in Fig. S6 (Supporting Information). Meanwhile, the absence of a strong intermolecular acting force will allow slipping of the molecular stacks upon exposure to external mechanical stimulus. When solid powder **1** is ground, a metastable amorphous state is formed, and changes in weak intermolecular C-H···π and C-H···F interactions and the formation of intermolecular aurophilic interactions are responsible for the significative mechanochromism behavior of **1**[33].

Insert Figure 2

Insert Figure 3

Insert Figure 4

Insert Figure 5

Insert Figure 6

*3.5. Reversible thin-film vapochromic luminescence behavior of complex **1***

The thin-film vapochromic luminescence property of complex **1** was evaluated by PL spectroscopy. Luminogen **1** is highly soluble in common solvents, which allows convenient solution processing and the formation of thin film. The PL spectral changes of **1** in response to vapors of frequently-used volatile organic compounds (VOCs) are shown in Fig. 7. The thin film of **1** showed bright yellow-green luminescence with the $\lambda_{\max}$ at 530 nm. However, when the thin film was exposed to vapors of different VOCs, including dichloromethane, trichloromethane, tetrahydrofuran, 1,4-dioxane, benzene, acetone, toluene, acetonitrile, diethyl ether, ethyl acetate, *etc*., the yellow emission with the $\lambda_{\max}$ at around 578 nm was observed. This red-shifted emission is related to that observed in the solid state emission (Fig. 2). The existence of different solvents molecules possibly resulted in the formation of intermolecular acting force, which altered the molecular stacking and intermolecular distance between the shortest Au atoms, and then changed the emission color from green to yellow [29]. Furthermore, the initial yellow-green emission reappeared when the thin film was removed from the different VOCs vapors. Thus, luminogen **1** also exhibited reversible vapochromic luminescence behavior.

Insert Figure 7

4. Conclusions

We report a carbazole-based mononuclear gold(I) complex. The complex is an interesting luminophor as it exhibits obvious AIE behavior, and its solid sample can emit persistent room-temperature phosphorescence with luminescence lifetime up to 86.84 ms, which is the highest lifetime value among all the reported gold(I) complexes so far. In addition, the luminogen also shows reversible high-contrast mechanochromism and vapochromism characteristics. To the best of our knowledge, this mononuclear gold(I) complex is the first example of an AIE-active luminogen with persistent room-temperature phosphorescence, reversible mechanochromic and vapochromic behaviors. It is believed that the multifunctional gold(I) complex will be outstanding candidate in the field of multistimuli-responsive materials. Furthermore, this work will also be beneficial to the design of new AIE-active metal-bearing luminogens with multistimuli-responsive behaviors and persistent room-temperature phosphorescence characteristics. Further explorations of gold(I) complexes with other significative properties are in progress.

Acknowledgments

The authors are grateful for the financial support from the National Natural Science Foundation of China (51373072, 201362013, 21662015, and 21472059), the Project of Jiangxi Sci-Tech Innovative Team (20142BCB24012), the Project of Jiangxi Academic and Technological leader (20142BCB22010), and the Project of the Science Fund of Jiangxi Education Office (GJJ160764).

Supporting Information Available

UV/visible-absorbance spectra of complex **1** (1.0 × 10^{-5} mol L^{-1}) in DMF-H_2O mixtures with different water contents. Size distribution curves of complex **1** (1.0 × 10^{-5} mol L^{-1}) in DMF-water mixtures with 60% and 90% volume fractions of water. SEM images and characterization data mentioned in the paper. Details of the crystal data collection, and selective bond lengths and angles.

References

[1] Nishino K, Yamamoto H, Tanaka K, Chujo Y. Development of solid-state emissive materials based on multifunctional *o*-carborane-pyrene dyads. Org Lett 2016;18:4064-7.

[2] Yang J, Huang J, Li Q, Li Z. Blue AIEgens: approaches to control the intramolecular conjugation and the optimized performance of OLED devices. J Mater Chem C 2016;4: 2663-84.

[3] Chen Z, Wu D, Han X, Liang J, Yin J, Yu GA, et al. A novel fluorene-based gold(I) complex with aggregate fluorescence change: a single-component white light-emitting luminophor. Chem Commun 2014;50:11033-5.

[4] Kishimura A, Yamashita T, Yamaguchi K, Aida T. Rewritable phosphorescent paper by the control of competing kinetic and thermodynamic self-assembling events. Nat Mater 2005;4: 546-9.

[5] Dong Y, Xu B, Zhang J, Tan X, Wang L, Chen J, et al. Piezochromic luminescence based on the molecular aggregation of 9,10-bis((*E*)-2-(pyrid-2-yl)vinyl)anthracene.

Angew Chem Int Ed 2012;51:10782-5.

[6] Chi Z, Zhang X, Xu B, Zhou X, Ma C, Zhang Y, et al. Recent advances in organic mechanofluorochromic materials. Chem Soc Rev 2012;41:3878-96.

[7] Xu B, Mu Y, Mao Z, Xie Z, Wu H, Zhang Y, et al. Achieving remarkable mechanochromism and white-light emission with thermally activated delayed fluorescence through the molecular heredity principle. Chem Sci 2016;7:2201-6.

[8] Patra A, Pan M, Friend CS, Lin TC, Cartwright AN, Prasad PN, et al. Electroluminescence properties of systematically derivatized organic chromophores containing electron donor and acceptor groups. Chem Mater 2002;14:4044-8.

[9] Ciardelli F, Ruggeri G, Pucci A. Dye-containing polymers: methods for preparation of mechanochromic materials. Chem Soc Rev 2013;42:857-70.

[10] Sagara Y, Yamane S, Mitani M, Weder C, Kato T. Mechanoresponsive luminescent molecular assemblies: an emerging class of materials. Adv Mater 2016;28:1073-95.

[11] Xue S, Qiu X, Sun Q, Yang W. Alkyl length effects on solid-state fluorescence and mechanochromic behavior of small organic luminophores. J Mater Chem C 2016;4:1568-78.

[12] Harada N, Abe Y, Karasawa S, Koga N. Polymorphic equilibrium responsive thermal and mechanical stimuli in light-emitting crystals of *N*-methylaminonaphthyridine. Org Lett 2012;14:6282-5.

[13] Mansour MA, Connick WB, Lachicotte RJ, Gysling HJ, Eisenberg R. Linear chain Au(I) dimer compounds as environmental sensors: a luminescent switch for the

detection of volatile organic compounds. J Am Chem Soc 1998;120:1329-30.

[14] Che Y, Yang X, Loser S, Zang L. Expedient vapor probing of organic amines using fluorescent nanofibers fabricated from an n-type organic semiconductor. Nano Lett 2008;8:2219-23.

[15] Nie H, Zhao Y, Zhang M, Ma Y, Baumgarten M, Müllen, K. Detection of TNT explosives with a new fluorescent conjugated polycarbazole polymer. Chem Commun 2011;47:1234-6.

[16] Wenger OS. Vapochromism in organometallic and coordination complexes: chemical sensors for volatile organic compounds. Chem Rev 2013;113:3686-733.

[17] White-Morris RL, Olmstead MM, Balch AL. Aurophilic interactions in cationic gold complexes with two isocyanide ligands. polymorphic yellow and colorless forms of [(cyclohexyl isocyanide)$_2$Au^I](PF$_6$) with distinct luminescence. J Am Chem Soc 2003;125:1033-40.

[18] Zhang X, Li B, Chen ZH, Chen ZN. Luminescence vapochromism in solid materials based on metal complexes for detection of volatile organic compounds (VOCs). J Mater Chem 2012;22:11427-41.

[19] Xia H, Liu D, Song K, Miao Q. Vapochromic and semiconducting solids of a bifunctional hydrocarbon. Chem Sci 2011;2:2402-6.

[20] Kim HJ, Whang DR, Gierschner J, Lee CH, Park SY. High-contrast red-green-blue tricolor fluorescence switching in bicomponent molecular film. Angew Chem Int Ed 2015;54:4330-3.

[21] Mei J, Leung NLC, Kwok RTK, Lam JWY, Tang BZ. Aggregation-induced

emission: together we shine, united we soar! Chem Rev 2015;115:11718-940.

[22] Luo J, Xie Z, Lam JWY, Cheng L, Chen H, Qiu C, et al. Aggregation-induced emission of 1-methyl-1,2,3,4,5-pentaphenylsilole. Chem Commun 2001;1740-1.

[23] Hutchings GJ, Brust M, Schmidbaur H. Gold-an introductory perspective. Chem Soc Rev 2008;37:1759-65.

[24] Gil-Rubio J, Cámara V, Bautista D, Vicente J. Dinuclear alkynyl gold(I) complexes containing bridging N-heterocyclic dicarbene ligands: new synthetic routes and luminescence. Organometallics 2012;31:5414-26.

[25] Wong WY, Choi KH, Lu GL, Shi JX, Lai PY, Chan SM, et al. Binuclear gold(I) and mercury(II) derivatives of diethynylfluorenes. Organometallics 2001;20:5446-54.

[26] Hunks WJ, Jennings MC, Puddephatt RJ. Self-association in gold chemistry: a tetragold(I) complex linked by both aurophilic and hydrogen bonding. Inorg Chem 2000;39:2699-702.

[27] Lu W, Kwok WM, Ma C, Chan CTL, Zhu MX, Che CM. Organic triplet excited states of gold(I) complexes with oligo(*o*- or *m*-phenyleneethynylene) ligands: conjunction of steady-state and time-resolved spectroscopic studies on exciton delocalization and emission pathways. J Am Chem Soc 2011;133:14120-35.

[28] Chen Z, Zhang J, Song M, Yin J, Yu GA, Liu SH. A novel fluorene-based aggregation-induced emission (AIE)-active gold(I) complex with crystallization-induced emission enhancement (CIEE) and reversible mechanochromism characteristics. Chem Commun 2015;51:326-9.

[29] Chen Z, Liang J, Nie Y, Xu X, Yu GA, Yin J, et al. A novel carbazole-based

gold(I) complex with interesting solid-state, multistimuli-responsive characteristics. Dalton Trans 2015;44:17473-7.

[30] Chen Z, Li Z, Hu F, Yu GA, Yin J, Liu SH. Novel carbazole-based aggregation-induced emission-active gold(I) complexes with various mechanofluorochromic behaviors. Dyes Pigm 2016;125:169-78.

[31] Ito H, Muromoto M, Kurenuma S, Ishizaka S, Kitamura N, Sato H, et al. Mechanical stimulation and solid seeding trigger single-crystal-to-single-crystal molecular domino transformations. Nat Commun 2013;4:2009-13.

[32] Benavente R, Espinet P, Lentijo S, Martín-Álvarez JM, Miguel JA, Rodríguez-Medina MP. Synthesis and characterization of gold(I) complexes with 9-(4-isocyanophenyl)carbazole or 9-ethyl-3-isocyanocarbazole ligands. Eur J Inorg Chem 2009;2009:5399-406.

[33] Liang J, Chen Z, Xu L, Wang J, Yin J, Yu GA, et al. Aggregation-induced emission-active gold(I) complexes with multi-stimuli luminescence switching. J Mater Chem C 2014;2:2243-50.

[34] Chen Z, Li Z, Yang L, Liang J, Yin J, Yu GA, et al. Novel diisocyano-based dinuclear gold(I) complexes with aggregation-induced emission and mechanochromism characteristics. Dyes Pigm 2015;121:170-7.

[35] Chen Z, Huang PS, Li Z, Yin J, Yu GA, Liu SH. Triisocyano-based trinuclear gold(I) complexes with aggregation-induced emission (AIE) and mechanochromic luminescence characteristics. Inorg Chim Acta 2015;432:192-7.

[36] Zou Y, Ye T, Ma D, Qin J, Yang C. Star-shaped

hexakis(9,9-dihexyl-9*H*-fluoren-2-yl)benzene end-capped with carbazole and diphenylamine units: solution-processable, high T_g hole-transporting materials for organic light-emitting devices. J Mater Chem 2012;22:23485-91.

[37] Luo J, Gong S, Gu Y, Chen T, Li Y, Zhong C, et al. Multi-carbazole encapsulation as a simple strategy for the construction of solution-processed, non-doped thermally activated delayed fluorescence emitters. J Mater Chem C 2016;4:2442-6.

[38] Sundar VC, Zaumseil J, Podzorov V, Menard E, Willett RL, Someya T, et al. Elastomeric transistor stamps: reversible probing of charge transport in organic crystals. Science 2004;303:1644-6.

[39] Guo Y, Yu G, Liu Y. Functional organic field-effect transistors. Adv Mater 2010;22:4427-47.

[40] Han A, Du P, Sun Z, Wu H, Jia H, Zhang R, et al. Reversible mechanochromic luminescence at room temperature in cationic platinum(II) terpyridyl complexes. Inorg Chem 2014;53:3338-44.

[41] Kitani N, Kuwamura N, Tsukuda T, Yoshinari N, Konno T. Counteranion-dependent mechanochromism of a photoluminescent platinum(II) complex with mixed terpyridine and thioglucose. Chem Commun 2014;50:13529-32.

[42] Morris WA, Liu T, Fraser CL. Mechanochromic luminescence of halide-substituted difluoroboron β-diketonate dyes. J Mater Chem C 2015;3:352-63.

[43] Zhen CG, Chen ZK, Liu QD, Dai YF, Shin RYC, Chang SY, et al. Fluorene-based oligomers for highly efficient and stable organic blue-light-emitting diodes. Adv

Mater 2009;21:2425-9.

[44] Uson R, Laguna A, Laguna M, Briggs DA, Murray HH, Fackler JP. (Tetrahydrothiophene)gold(I) or gold(III) complexes. Inorg Synth 1989;26:85-91.

[45] Sheldrick GM. SHELXS-97, a program for crystal structure solution. 1997. Germany: Göttingen.

[46] Sheldrick GM. SHELXL-97, a program for crystal structure refinement. 1997. Germany: Göttingen.

[47] Leung CWT, Hong Y, Chen S, Zhao E, Lam JWY, Tang BZ. A photostable AIE luminogen for specific mitochondrial imaging and tracking. J Am Chem Soc 2013;135:62-5.

[48] Jiang Y, Wang Y, Hua J, Tang J, Li B, Qian S, et al. Multibranched triarylamine end-capped triazines with aggregation-induced emission and large two-photon absorption cross-sections. Chem Commun 2010;46:4689-91.

[49] Hong Y, Lam JWY, Tang BZ. Aggregation-induced emission: phenomenon, mechanism and applications. Chem Commun 2009;4332-53.

[50] Liang J, Chen Z, Yin J, Yu GA, Liu SH. Aggregation-induced emission (AIE) behavior and thermochromic luminescence properties of a new gold(I) complex. Chem Commun 2013;49:3567-9.

[51] Ito H, Saito T, Oshima N, Kitamura N, Ishizaka S, Hinatsu Y, et al. Reversible mechanochromic luminescence of [$(C_6F_5Au)_2$(μ-1,4-diisocyanobenzene)]. J Am Chem Soc 2008;130:10044-5.

[52] Zhang G, Palmer GM, Dewhirst MW, Fraser CL. A dual-emissive-materials

design concept enables tumour hypoxia imaging. Nat Mater 2009;8:747-51.

[53] Bolton O, Lee K, Kim HJ, Lin KY, Kim J. Activating efficient phosphorescence from purely organic materials by crystal design. Nat Chem 2011;3:205-10.

[54] Bergamini G, Fermi A, Botta C, Giovanella U, Motta SD, Negri F, et al. A persulfurated benzene molecule exhibits outstanding phosphorescence in rigid environments: from computational study to organic nanocrystals and OLED applications. J Mater Chem C 2013;1:2717- 24.

[55] Yang Z, Mao Z, Zhang X, Ou D, Mu Y, Zhang Y, et al. Intermolecular electronic coupling of organic units for efficient persistent room-temperature phosphorescence. Angew Chem Int Ed 2016;55:2181-5.

Table of Contents

1. **Chart 1.** (a) The structure of complex **1**. (b) The configuration of a gold(I) complex molecule taken form the single crystal structure.

2. **Scheme 1.** Synthetic route to the carbazole-based gold(I) complex **1**.

3. **Figure 1.** (a) Photoluminescence (PL) spectra of the dilute solutions of luminogen **1** (1.0×10^{-5} mol L^{-1}) in a mixture of DMF-H_2O with different water contents (0-60%). Excitation wavelength = 330 nm. The inset shows the emission images of **1** (1.0×10^{-5} mol L^{-1}) in pure DMF, 50% water fraction and 60% water fraction under irradiation with UV light at 365 nm. (b) PL spectra of the dilute solutions of luminogen **1** (1.0×10^{-5} mol L^{-1}) in a mixture of DMF-H_2O with various water contents (60-90%). Excitation wavelength = 330 nm. The inset shows the emission

images of **1** (1.0×10^{-5} mol L^{-1}) in 60% water fraction as well as 90% water fraction under irradiation with UV light at 365 nm.

4. **Figure 2.** (a) Solid-state PL spectra of complex **1** before grinding, after grinding, and after treatment with dichloromethane solvent vapor. Excitation wavelength: 365 nm. Photographic images of **1** under 365 nm UV light: (b) the as-synthesized solid sample. (c) the ground solid sample. (d) the solid sample after treatment with dichloromethane solvent vapor.

5. **Figure 3.** Decay curve of the gold(I) complex at the peak emission wavelength of 550 nm. Excitation wavelength: 365 nm.

6. **Figure 4.** Reversible change in PL peak intensity (538 nm) of the gold(I) complex recorded for several grinding-fuming processes.

7. **Figure 5.** X-ray diffraction (XRD) patterns of gold(I) complex **1** in different solid states: the as-prepared solid, the ground powder and the solid after treating the ground sample with dichloromethane vapor.

8. **Figure 6.** The molecular packing of the coordination compound **1** in a single crystal cell. The dashed lines are showing the distances between the correlation atoms in the crystal. The H, C, N, F, and Au atoms are colored in light grey, dark grey, blue, yellow and pink, respectively.

9. **Figure 7.** (a) Emission spectra of luminogen **1** thin film, exposed to different VOCs vapors and away from different VOCs vapors. Excitation wavelength: 365 nm. (b) Photographic images of **1** thin film, exposed to different VOCs vapors and away from different VOCs vapors under 365 nm UV light.

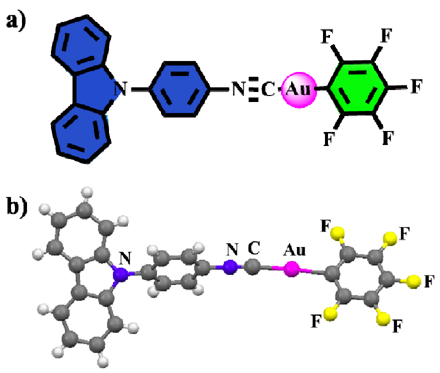

Chart 1. (a) The structure of complex **1**. (b) The configuration of a gold(I) complex molecule taken form the single crystal structure.

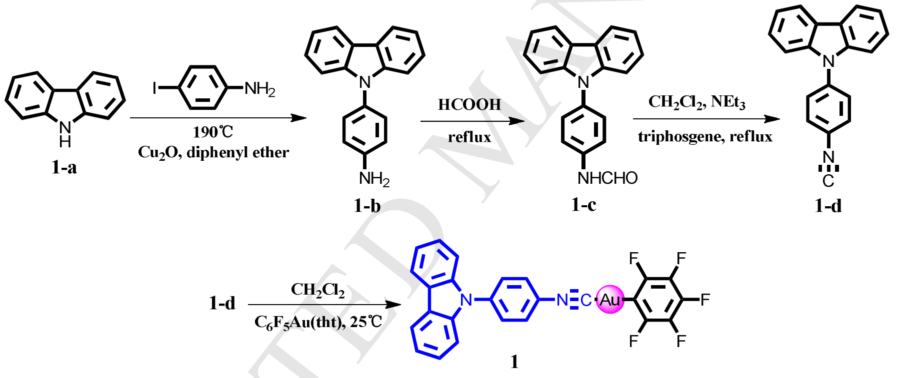

Scheme 1. Synthetic route to the carbazole-based gold(I) complex **1**.

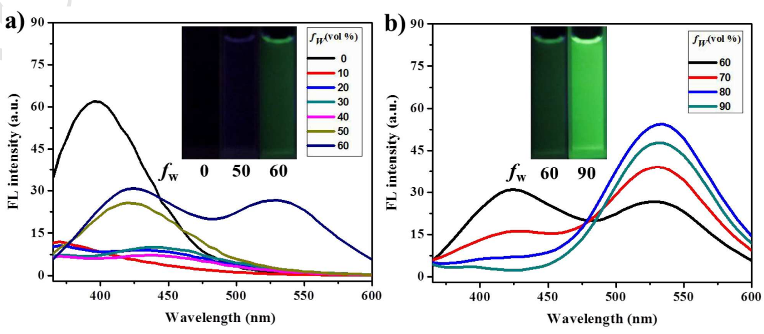

Figure 1. (a) Photoluminescence (PL) spectra of the dilute solutions of luminogen **1** (1.0×10^{-5} mol L^{-1}) in a mixture of DMF-H_2O with different water contents (0-60%). Excitation wavelength = 330 nm. The inset shows the emission images of **1** (1.0×10^{-5} mol L^{-1}) in pure DMF, 50% water fraction and 60% water fraction under irradiation with UV light at 365 nm. (b) PL spectra of the dilute solutions of luminogen **1** (1.0×10^{-5} mol L^{-1}) in a mixture of DMF-H_2O with various water contents (60-90%). Excitation wavelength = 330 nm. The inset shows the emission images of **1** (1.0×10^{-5} mol L^{-1}) in 60% water fraction as well as 90% water fraction under irradiation with UV light at 365 nm.

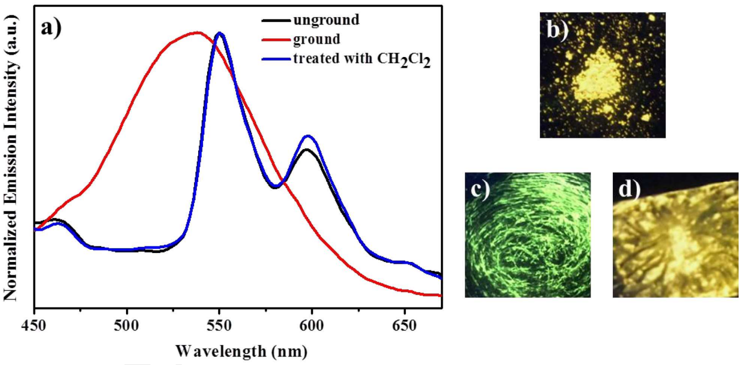

Figure 2. (a) Solid-state PL spectra of complex **1** before grinding, after grinding, and after treatment with dichloromethane solvent vapor. Excitation wavelength: 365 nm. Photographic images of **1** under 365 nm UV light: (b) the as-synthesized solid sample. (c) the ground solid sample. (d) the solid sample after treatment with dichloromethane solvent vapor.

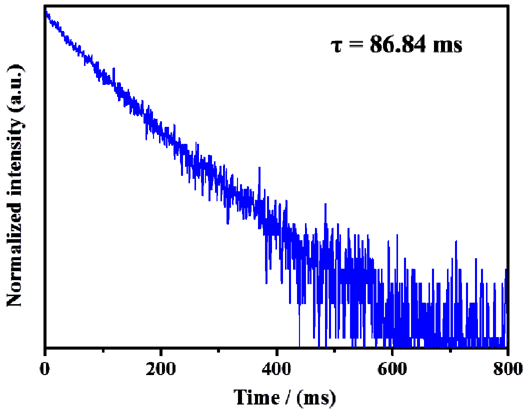

Figure 3. Decay curve of the gold(I) complex at the peak emission wavelength of 550 nm. Excitation wavelength: 365 nm.

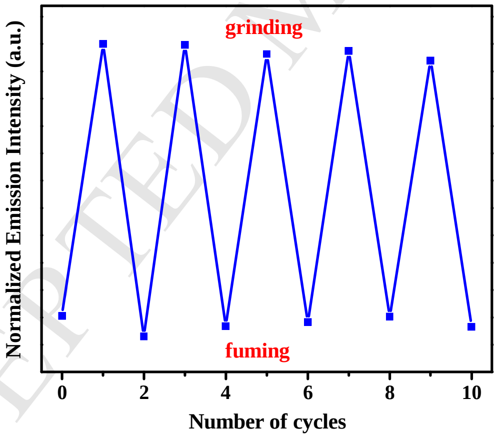

Figure 4. Reversible change in PL peak intensity (538 nm) of the gold(I) complex recorded for several grinding-fuming processes.

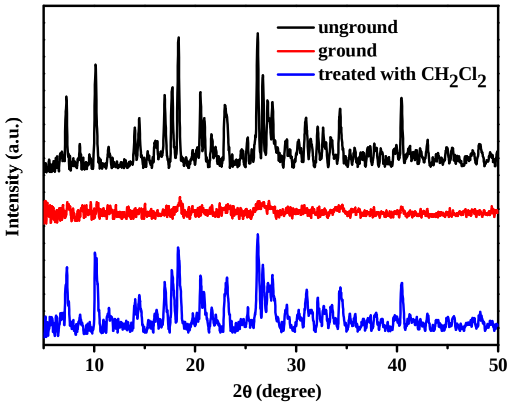

Figure 5. X-ray diffraction (XRD) patterns of gold(I) complex **1** in different solid states: the as-prepared solid, the ground powder and the solid after treating the ground sample with dichloromethane vapor.

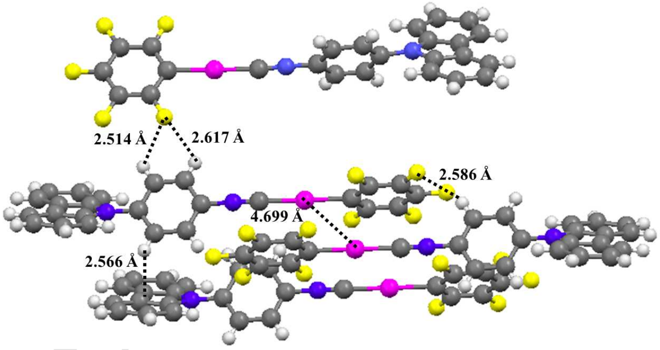

Figure 6. The molecular packing of the coordination compound **1** in a single crystal cell. The dashed lines are showing the distances between the correlation atoms in the crystal. The H, C, N, F, and Au atoms are colored in light grey, dark grey, blue, yellow and pink, respectively.

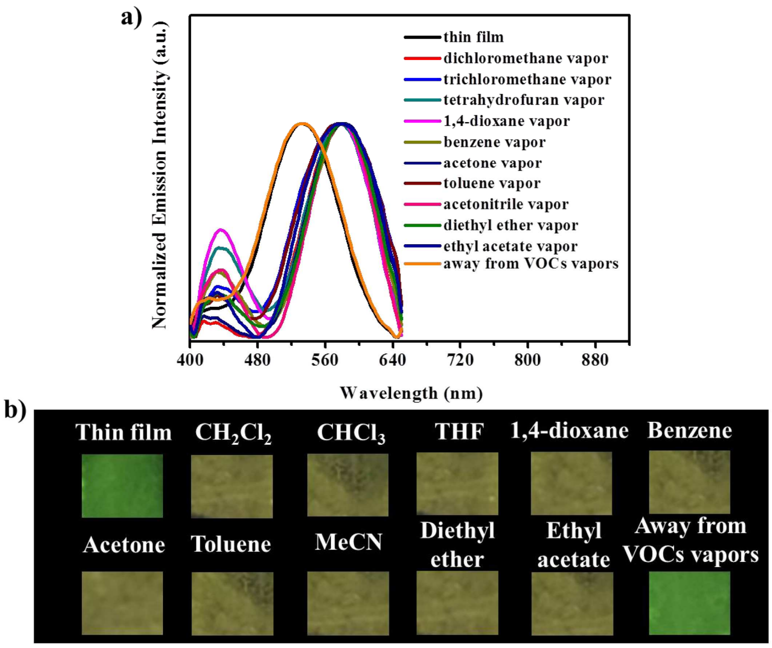

Figure 7. (a) Emission spectra of luminogen **1** thin film, exposed to different VOCs vapors and away from different VOCs vapors. Excitation wavelength: 365 nm. (b) Photographic images of **1** thin film, exposed to different VOCs vapors and away from different VOCs vapors under 365 nm UV light.

Highlights

- A carbazole-based mononuclear gold(I) complex was synthesized.
- The gold(I) complex exhibits obvious aggregation-induced emission (AIE) property.
- The gold(I) complex can emit persistent room-temperature phosphorescence with a solid-state emission lifetime up to 86.84 ms.
- The gold(I) complex shows reversible mechanochromic luminescence behavior.
- The gold(I) complex shows reversible vapochromic luminescence behavior.